ASEAN Engineering Journal

Full Paper

COMPONENT-BASED SEVERE WIND VULNERABILITY ANALYSIS OF WOODEN BUILDINGS IN THE PHILIPPINES

Joshua C. Agar, Joshua Joseph C. Gumaro, Timothy John S. Acosta*, John Phillip G. Alvarez, Mary Nathalie C. Ereño, Jaime Y. Hernandez Jr. , Jihan S. Pacer, Dean Ashton D. Plamenco, Liezl Raissa E. Tan, Julius Baniqued, Eric Augustus J. Tingatinga, John Kenneth B. Musico, Pher Errol B. Quinay, Imee Bren O. Villalba, Harvey O. Bisa

Institute of Civil Engineering, University of the Philippines Diliman, Quezon City, Philippines

Article history
Received
11 August 2021
Received in revised form
10 December 2021
Accepted
12 December 2022
Published online
31 May 2022

*Corresponding author
tsacosta@up.edu.ph
r

Graphical abstract

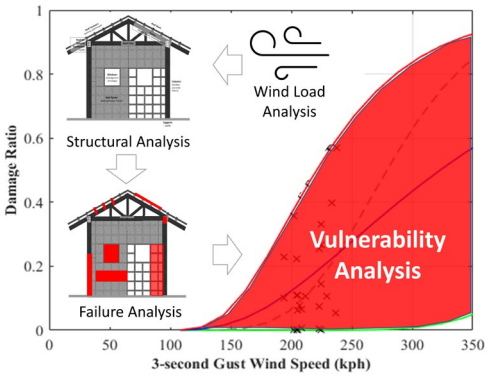

Abstract

The Northwestern Pacific Ocean Basin is home to the strongest tropical cyclones in the world, called typhoons. The Philippines is situated as the gateway for the typhoons developing in the Northwestern Pacific Basin. As a result, the country is being exposed to the risk brought by significantly strong typhoons that occur more than once annually. Lightweight buildings, particularly wooden buildings, and their structural components are the most vulnerable to severe winds. This study aims to perform vulnerability analysis on wooden buildings, by developing vulnerability curves that relate the magnitude of severe winds to the variation of damages and by establishing the probabilities of identified damage states of the buildings at certain wind speeds - which are called fragility curves. This study employs an improved framework from a heuristic-empirical-computational methodology previously used in determining GMMA-RAP vulnerability curves. This enhanced framework uses a component-based Monte Carlo vulnerability analysis to determine the improved vulnerability curve to account for the statistical variations of documented building damage from severe winds. A maximum, average, and minimum vulnerability curve were developed by fitting a cumulative lognormal distribution function wherein the mean parameters are 250.92, 425.89, 148.80, and the variance parameters are 0.579, 0.257, 0.433, respectively—the functions used an offset of 72 kph for all the developed curves. The developed curves were then compared to empirical field survey data, wherein 71.43% of the empirical data was within the developed envelope.

Keywords: Severe Wind, Vulnerability, Analysis, Wooden, Buildings, Philippines

© 2022 Penerbit UTM Press. All rights reserved

1.0 INTRODUCTION

The Philippines is prone to severe wind risk brought about by typhoons that frequently affect the island nation. The nation's weather agency, the Philippine Atmospheric, Geophysical, and Astronomical Services Administration (PAGASA) records an average of 20 typhoons being monitored annually [1].

Being exposed to the risk brought by earthquakes, residents opt for lightweight materials, mainly wood, in construction to reduce the risk of damage or collapse. However, this, in turn, makes the residential houses more vulnerable to typhoons instead.

Wooden buildings are often found in rural areas, which are more exposed to typhoons' severe winds. Being subjected to these unfavorable conditions, repairs would be costly for the residents if they were caught unaware of the risk brought by severe winds. Therefore, as part of the severe wind risk evaluation, evaluating the vulnerability would lead to mitigation and preparedness.

Mainly made of wooden materials, wooden buildings exhibit repetitive roof framing by wooden rafters or trusses, repetitive wall framing by wood studs. To resist the lateral loads, the roof panels, floor sheathings, and wall sheathing act as diaphragms to transfer the loads to the walls and roof framing. For single-story wooden houses, the floor can either be a

concrete slab on the ground level or a wooden floor supported by wooden stilts.

Typhoon Yolanda (International Name: Haiyan) in 2013 served as a wake-up call to realizing the full extent of the risk of severe winds brought by typhoons as it brought extensive devastation along its path [2]. As a result, extensive research ventured into severe wind risk assessment apart from the severe wind speed maps update. Following the pattern for risk analysis detailed by the Federal Emergency Management Agency (FEMA) in the multi-hazard tool that they developed named HAZUS [3], the University of the Philippines Diliman Institute of Civil Engineering (UPD-ICE) developed preliminary fragility and vulnerability curves in 2014 for multi-hazard, including severe wind, for the greater Metro Manila Area. [4]. Figure 1 shows the vulnerability curve while Figure 2 shows the fragility curves for wooden buildings developed in 2014. The vulnerability curve is fitted from the averages of documented damage at different wind speed increments, while the fragility curves are fitted from the documented probabilities of exceedance of damage states [4].

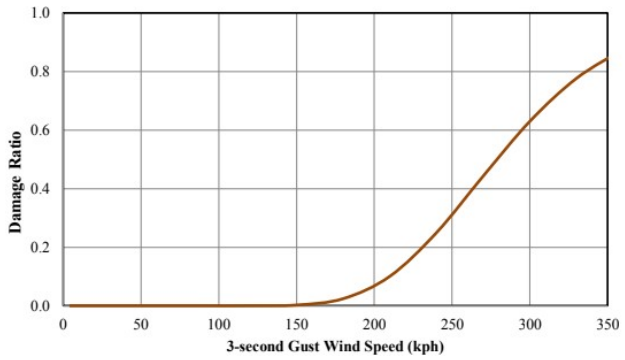

Figure 1 UPD-ICE developed vulnerability curve for Wooden Buildings (W1) in 2014.

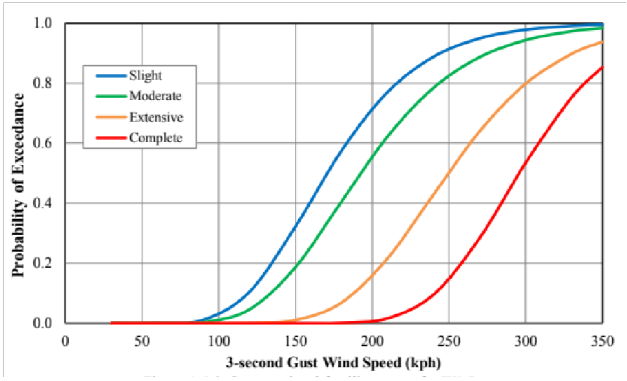

Figure 2 UPD-ICE developed fragility curves for Wooden Buildings (W1) in 2014.

The Greater Metro Manila Area - Risk Analysis Project (GMMA-RAP) is the precedent of the current pilot study involving government agencies and institutions like PAGASA, UPD-ICE, and the Philippine Institute of Volcanology and Seismology (PHIVOLCS), with the province of Cebu as the pilot area. The previous GMMA curves resulted from a mix of computational, heuristic, and empirical analysis. Expert opinions constituted the heuristic component. Documented building damage from field surveys included the empirical component. Simulated component failure due to wind pressure constituted the computational component of the analysis. The study aims to provide a newer and more rigorous iteration of the vulnerability analysis for wooden buildings. Recent research [5] has also discussed the methodology used in this study to collect field survey data and identify key building components. From the previous wind pressure-based approach to damage simulation, this study improved the previous methodology by introducing a component-based approach previously implemented on concrete buildings with steel roof framing. The components of interest involve roof truss, roof-to-column connections, purlins, roof fasteners, and roof sheets in the failure simulation [6] to consider the propagation of failure and the statistical variations of documented damage ratios and even damage states.

In the following sections, we discuss the methodology conducted in the study. First, the representative building types were determined using clustering analysis from surveyed samples. Then, these representative building types were used in the structural analysis. The building capacities of the structural components were determined through experimentation. To determine the wind loading, computational fluid dynamics analysis was performed. Then, we discuss the failure propagation and vulnerability analysis employed in the study.

2.0 REPRESENTATIVE BUILDING TYPES

Among the 177 buildings surveyed in Cebu province, 23 of those buildings were identified as wooden buildings. These buildings are further classified into subgroups depending on their wall materials. Fourteen have plywood walls, six have woven bamboo (Sawali) as wall material, and three belong to wooden buildings that are the hybrid of the first two subgroups. Six representative building geometries were identified based on the building geometry parameters of the 23 surveyed buildings. Figure 3 shows the sample structural models used for different roof shapes.

Table 1 Dimensions of the representative geometries in the analysis

Parameter	Gable 1	Gable 3	Gable 5	Hip 1	Hip 3	Mono-slope 1
Height (m)	4.08	4.26	5.84	3.95	5.90	5.42
Length (m)	10.50	5.97	11.6	7.37	13.42	6.92
Width (m)	5.07	4.62	8.76	5.70	8.75	4.78
Roof Slope (deg)	15.33	19.00	19.50	24.20	21.03	8.83
Eaves Long (m)	1.010	0.850	0.675	0.825	1.030	0.700
Eaves Short (m)	0.500	0.580	0.575	0.700	0.875	0.200

The representative geometries were identified through the clustering analysis of the building stock geometry of the surveyed buildings, where statistical geometric similarity identified clusters in the building population [7]. The representative geometries shown in Table 1 were then derived from the identified clusters in the building population.

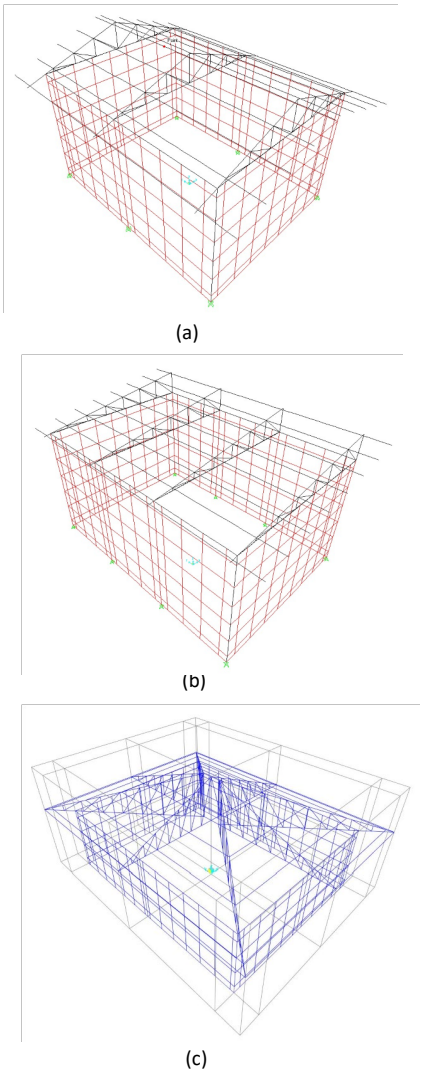

Figure 3 Structural models generated for (a) gable, (b) mono slope, and (c) hip roof buildings

3.0 BUILDING COMPONENT CAPACITIES

This study has previously identified vulnerable components such as walls and supports for non-engineered wooden buildings [5,8]. Therefore, different Failure states of the columns, such as bending failure and shear failure, which mainly depend on the properties of the wooden material used, were also considered in the analysis. The wooden material was assumed to be either good lumber or coconut lumber, having bending capacities of 20.625 MPa [9] and 15.4 MPa [10], respectively.

The wood material used can also cause differences in the pull-out strength of roof fasteners. For coco lumber, an average pull-out strength of 433.50 N was observed [11], while the average pull-out strength for good lumber was 656 N [8]. The resistance capacities used in this study for the purlin connection, supports, wall, and window materials were gathered from recent literature [5,12,13,14]. In addition, each of the 23 buildings has its own unique set of building geometries, structural framing, fastener spacing, and building components, whose capacities are determined through a series of material tests, as listed in Table 2

Table 2 Resistance capacities of components

Component	Component Type	Mean Capacity	Coefficient of Variance	References
(x2) 3 in Nail	Purlin Connection	6500.00 N	0.07	[12]
(x6) Bent Nails	Supports	7777.10 N	0.10	[12]
(x4) Bent Nails	Supports	5184.73 N	0.13	[12]
Umbrella Nail	Roof Fastener	656.00 N (Good lumber) 433.50 N (Coconut Lumber)	0.68 (Good lumber) 0.21 (Coconut Lumber)	[8] [11]
Plywood	Wall Material	2.88 kPa	0.27	[12]
Tongue-and-groove	Wall Material	17.43 kPa	0.25	[12]
Woven Bamboo (Sawali)	Wall Material	4.27 kPa	0.14	[12]
Sliding Wood	Window Material	3.51 kPa	0.16	[12]
Sliding Glass	Window Material	2.37 kPa	0.27	[12]
Wood Jalousie	Window Material	86.41 kPa	0.34	[14]
Glass Jalousie	Window Material	4.22 kPa	0.23	[13]
Fixed Glass	Window Material	4.07 kPa	0.33	[12]

4.0 CFD ANALYSIS

Using Computational Fluid Dynamics (CFD), the wind flow was simulated around the building envelope of the representative buildings assumed to be in isolated conditions. The parameters of the CFD analysis, including the discretization of the domain, were optimized through validation using a comparative analysis involving the aerodynamic response of the buildings subjected to wind tunnel analysis by Tokyo Polytechnic University (TPU) [15], in terms of non-dimensional constants called the Coefficients of pressure. The validation procedure also included a mesh sensitivity analysis resulting in an optimized mesh shown in Figure 4.

As shown in Figure 5, the validation procedure also included a comparative analysis of the RANS turbulence models to determine which model would result in simulated coefficients of pressure closest to wind tunnel values. The Renormalization Group (RNG) k-epsilon model [16] was deemed the most optimal turbulence model among the RANS turbulence models. After the validation procedure, the aerodynamic loads were extracted from the CFD analysis of the building archetypes listed in Table 1. The mesh optimization procedure was applied to the representative building geometries in this study. Finally, the simulated wind pressure coefficients were used to determine the different loadings on the structural models.

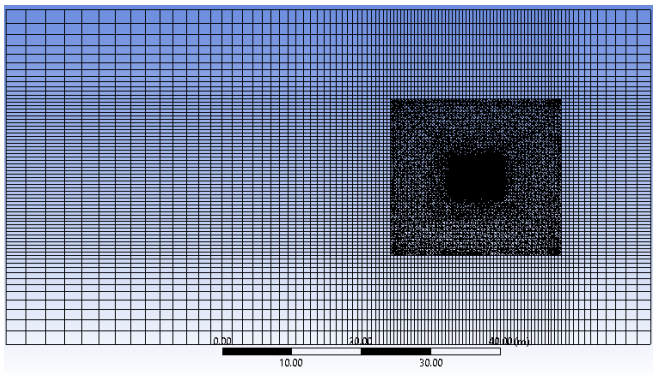

(a)

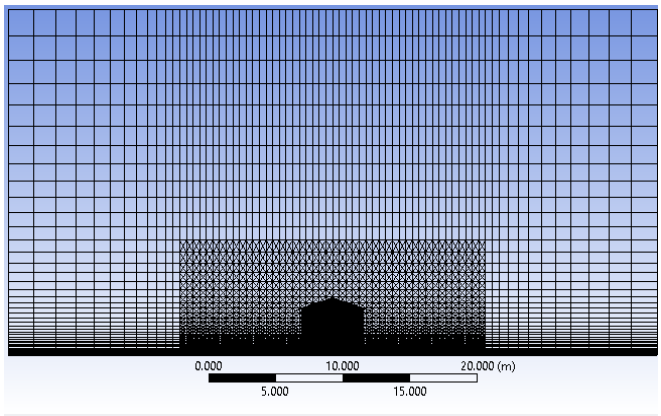

(b)

Figure 4 (a) Top view and (b) front view of sample discretization of computational domain for CFD analysis

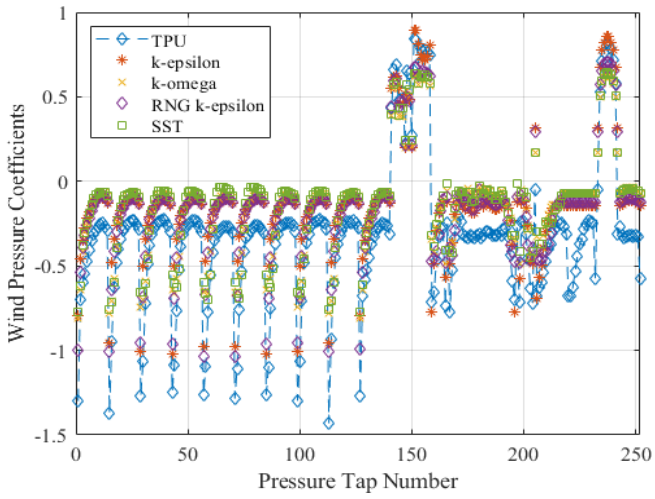

Figure 5 Validation of the CFD analysis with the TPU wind tunnel tests

5.0 FAILURE PROPAGATION

This study considered the propagation of damage as detailed in Figure 7 for the key building components shown in figure 6. For example, suppose the foundations experience failure at a given wind load case. In that case, it will lead to structural instability and subsequent failure of the portions of the walls supported by these foundations. Also, the failure of certain foundations will propagate to the columns being supported.

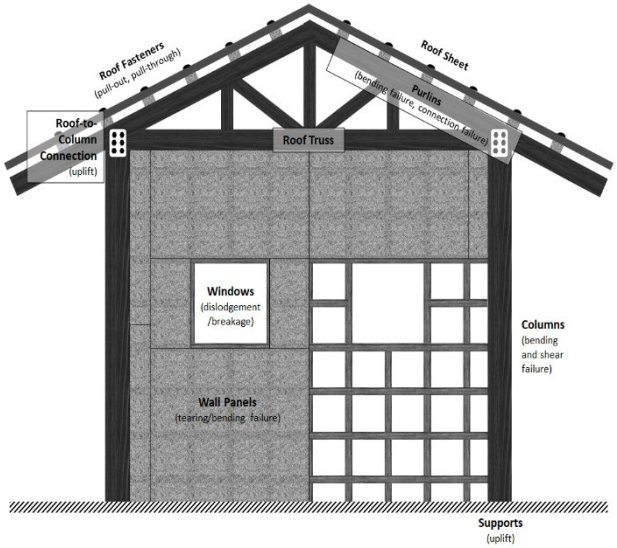

Figure 6 Identified key building components of wooden buildings

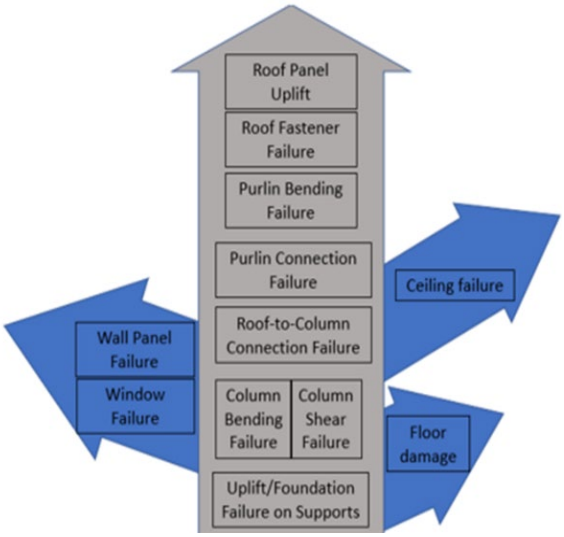

Figure 7 Hierarchy of failure propagation among the identified key building components

This study has identified a hierarchy within building components. Even if the wind loads acting on a building component do not exceed its resistance capacity and another building component directly lower in the hierarchy fails, that affected building component is also considered to have failed. For example, if onset damage occurs in the columns or their supports, the damage from the columns will then propagate to their corresponding roof-to-column connections and so on, as shown in Figure 7.

The aerodynamic loads were then transmitted through the buildings, where a subsequent structural analysis was performed to determine the internal forces among the components. With the CFD analysis and structure analysis determining the structural demand and the material tests determining the structural capacities, failure is observed for each component if the demand exceeds the capacity or the damage

propagated from a component higher in the hierarchy in Figure 7.

6.0 VULNERABILITY ANALYSIS

Since the strength capacities of the different components are statistical, Monte Carlo simulations were performed to cover the variations of strength capacities. A total of 23 buildings and a set of finite unique angles of attack resulted in 33,400 building cases for each increment of wind speed. Considering all the different cases mentioned, the internal loads developed were compared to their corresponding randomly generated strength for each building component. If the internal loads were greater than the strength capacities, the building component would be considered damaged for the certain building case considered.

The minimum and maximum envelope of the damage ratios, the cost of repairing the damaged components over the total construction costs, and the average values of these ratios were determined for each wind speed increment. Only those data points within two standard deviations from the average value at 95% confidence [5] were considered to remove the possible outliers, as shown in Figures 6 and 8. The minimum and maximum enclosure values and average values were then fitted into a cumulative lognormal distribution function with an offset of 72 kph (Equation 1).

Adopting the methodology in HAZUS [6], the damage state for roof cover, windows, roof structure, and walls were evaluated for each building case. The overall building damage state was determined by obtaining the highest damage state among the four components.

Compiling all the population containing each overall building damage state at each increment and fitting into Equation 1 will determine the fragility curves for each damage state.

$$Probability\ of\ Exceedance_{DS}(V) = CDF_{lognormal}(V\text{-}V_o,\mu,s) \quad (1)$$

Where V_0 is the offset of the cumulative distribution function (CDF) in kph, μ is the median or mean of the CDF in kph, σ is the standard deviation of the CDF.

The percent damage of each building component is also determined for each building case. Then, the damage per component is multiplied by the ratio of repair per component to the total construction cost to aggregate the component damages into one building damage ratio. This ratio is called the component cost factor (CCF). The equation used to determine the total damage ratio is shown in equation 2.

$$DR_{total} = \sum DR_i \text{ X } CCF_i \quad (2)$$

The key building components provided with CCF values for each key subtype in Table 3 are mainly divided into seven (7) components for three types of wooden buildings with different wall materials. The different types are wooden buildings with Sawali walls (SW), wooden walls (WW), and with a mix of wooden and Sawali walls (MWSW). These are the roof fasteners (RF), roof covering (RC), purlins (PS), roof structure (RS), exterior walls (EW), exterior doors & windows (EDW) and other vulnerable components (OT). Table 4 shows the equivalent construction cost per square meter for each component. The largest CCF among the components was under the classification OT (Vulnerable), which covered the repair cost of the main wooden columns and stilts (if present) and the wooden floors. The damage among these components will be counted if the supports suffer failure. Also, shown in Figure 5, the failure of the supports will also lead to the propagation of failure to the other building components, as it signifies structural collapse as observed in the field surveys. As a consequence, the failure of the supports will attribute to most of the building damage ratio, with the slope of the vulnerability curve expected to increase along with the increase of the probability of exceedance of the failure of the supports, which is classified as Damage State 4 based on the fragility curves proposed by the GMMA-RAP report [7].

Table 3 Component-cost factors of wooden buildings with different types of wall materials

Types	RF	RC	PS	RS	EW	EDW	OT
SW	0.0084	0.1672	0.0287	0.1329	0.2237	0.1580	0.3157
WW	0.0057	0.1042	0.0528	0.1007	0.2113	0.1165	0.4449
MWSW	0.0070	0.1660	0.0303	0.1332	0.1855	0.1777	0.3351

Table 4 Construction cost per square meter (Php/sqm) of wooden buildings with different types of wall materials

Types	RF	RC	PS	RS	EW	EDW	OT	Total
SW	35.85	713.37	122.40	566.93	954.22	674.07	1347.07	4266.28
WW	24.48	450.98	228.47	435.46	913.93	504.18	1924.92	4326.30
MWSW	26.66	635.07	115.86	509.60	709.44	679.60	1281.53	3824.60

7.0 VULNERABILITY CURVES

The vulnerability curves determined by this study statistically considered the variation of building component strengths, building geometries, and angles of wind approach. In addition, this study entails the inclusion of the curves for the minimum and maximum damage ratios to take into account the variability of scenarios that may arise during actual severe wind events. This results in the scatterplot of the damage ratios across wind speeds shown in Figure 8.

The recently developed maximum, average and minimum vulnerability curves allow different stakeholders to conduct various risk assessment scenarios to aid in implementing disaster risk reduction mitigation strategies. Previously developed curves such as the GMMA-RAP curves could not consider the variations in parameters, which led to only average vulnerability curves. Despite the difference, it can be observed that the computational GMMA-RAP vulnerability curves fall within the interval between the minimum and maximum scenario made by this study's vulnerability curves, as shown in Figure 8.

Figure 9, on the other hand, shows the corresponding fragility curves developed. Finally, the newly developed curves are superimposed on the GMMA-RAP computational vulnerability curves shown in Figure 8. On average, as shown in Figure 8, this study's average damage curve, when compared to the average damage curve from the GMMA-RAP curve, has greater damage ratios at wind speeds between 110 kph and 220 kph while having lesser damage ratios at wind speeds greater than 220 kph.

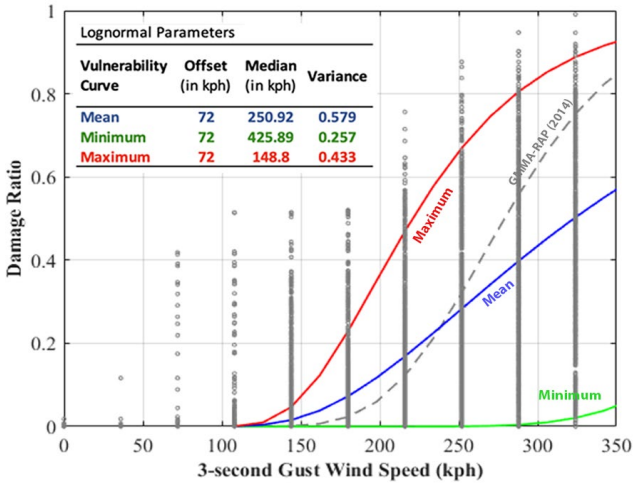

Figure 8 Corrected values for the minimum (green) and maximum (red) enclosures in contrat to the scatterplot of damage ratios of all W1 building cases

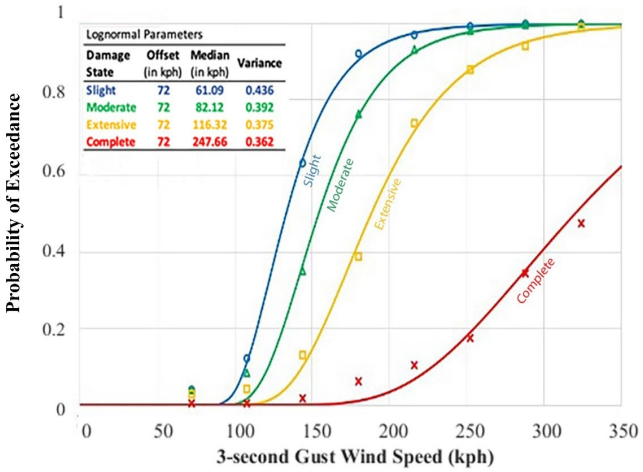

Figure 9 Fragility curves for wooden structures (W1-L)

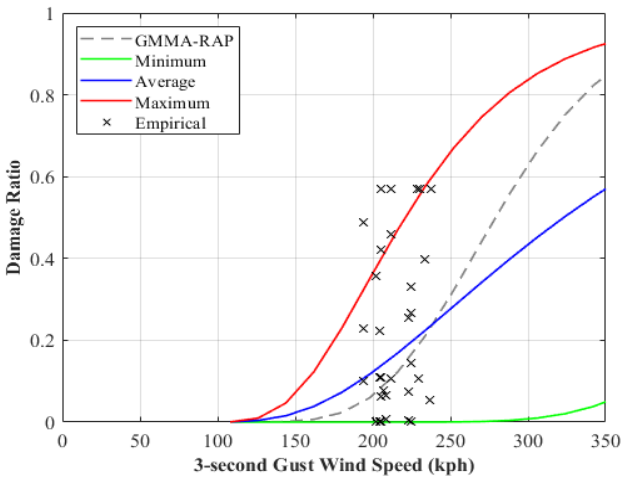

Figure 10 Comparison of the vulnerability curve with empirical data points from Typhoon Kammuri (2019)

8.0 VALIDATION OF RESULTS

The statistical nature of the enhanced curves of this study was also vital in capturing the variability of actual scenarios compared with the empirical data obtained during the field survey of the aftermath of Typhoon Kammuri (2019), plotted in Figure 10.

Figure 11 Photos of some of the surveyed buildings that exceeded the maximum damage ratio

Out of the 35 surveyed wooden buildings in the field survey, 25 samples fell within the envelope of the minimum damage curve and the maximum damage curve. Twenty-one samples did not exceed the upper limit imposed by the maximum damage ratio curves, with the three samples not experiencing any damage at all. This equates to a total of 71.43% of the empirical data being within the developed envelope.

The seven samples exceeding the maximum damage ratios, as shown in Figure 11, were observed to be either built on loose soil foundations or aged considerably. These observations are similar to recent studies [17] that investigated concrete school buildings with wooden roof structures in the Philippines, wherein buildings with deterioration due to aging and termites contribute significantly to outliers of empirical damaged data.

9.0 CONCLUSIONS AND RECOMMENDATIONS

This paper presents a vulnerability analysis for wooden buildings in the Philippines using a component-based methodology. The improved method uses a hierarchical approach for the propagation of damage from one component to another, wherein the damage is propagated from the supports of the columns vertically upwards to the roof panels. Wind loads for the analysis were determined using a computational fluid dynamics analysis. A Monte Carlo simulation was performed by evaluating the internal loads and probabilistic capacities of each component.

Considering the variability of building geometries, components, and structural configurations led to a wide range of damage ratios expected on the wooden buildings. The study has produced three vulnerability curves considering the components' variations that follow a cumulative lognormal distribution function. The lognormal parameters mean parameters are 250.92, 425.89, 148.80, and the variance parameters are 0.579, 0.257, 0.433, respectively—the functions used an offset of 72 kph for all the developed curves. In addition, a comparison of the computational curves to the survey data revealed the need to consider the soil foundations of the study and how aging affects the overall performance of the wooden buildings against severe winds. Finally, further statistical tests on validating simulation model results should be considered, especially when working

with small data sets from field observations. Overall, the study's vulnerability and fragility curves can be used to predict expected damage on wooden buildings as part of the risk analysis.

Acknowledgement

This study was conducted under the auspices of the project by the Department of Science and Technology (DOST) titled "Enhanced Severe Wind Vulnerability Curves of Key Building Types in the Philippines." The project was under a DOST program titled "Severe Wind Hazard and Risk Analysis of the Philippines," along with the Philippine Institute of Volcanology and Seismology and the Philippine Atmospheric, Geophysical and Astronomical Services Administration. They provided the wind speeds for the surveyed damaged buildings during Typhoon Kammuri (2019).

References

[1] McCurry, Justin. 2009 “Philippines Struggles to Recover From Typhoons.” Lancet

[2] Agar, Joshua, William Mata, and Jaime Jr. Hernandez. 2018. "Estimating Typhoon Haiyan's Wind Speeds Using Windicators." *Philippine Engineering Journal*, 39(1): 29-42.

[3] Schneider, Phillip, and Barbara Schauer. 2006."HAZUS—Its Development and Its Future." *Natural Hazards Rev.*, 7(2): 40-44,

[4] Pacheco, Benito, Jaime Jr. Hernandez, Peter Castro, Eric Tingatinga, Raniel Suiza, Liezl Tan,Romeo Longalong, Clarissa Veron, Harold Aquino, Richmark Macuha, William Mata, Imee Villalba, Claire Pascua, Ulpiano Jr. Ignacio, Fernando Germar, Joseph Diño, Gian Reyes, Lemar Tirao, and Mark Zarco. 2014. "Development of Vulnerability Curves of Key Building Types in the Greater Metro Manila Area, Philippines".

[5] Gumaro, Joshua Joseph C., Acosta, Timothy John S., Tan, Liezl Raissa E., Agar, Joshua C., Tingatinga, Eric Augustus J., Musico, John Kenneth B., Plamenco, Dean Ashton D., Ereño, Mary Nathalie C.,Pacer, Jihan S., Villalba, Imee Bren O. and Hernandez, Jaime Y. Jr. 2021"Identification of key components for developing building types for risk assessment against wind loadings: The case of Cebu Province, Philippines", International *Journal of Disaster Risk Reduction*. 64(2022): 102686. DOI: http://doi.org/10.1016/j.ijdrr.2021.102686

[6] Tan, Liezl. 2014. "Wind Vulnerability Assessment Of Enhanced Wind Resilient Design For A Standard 1-Storey School Building In Tacloban Using Component-Based Approach in Reliability Modeling". Graduate thesis,

[7] Tan, Liezl Raissa E., Acosta, Timothy John S., Gumaro, Joshua Joseph C.,Agar, Joshua C., Tingatinga, Eric Augustus J., Plamenco, Dean Ashton D.,Ereno, Mary Nathalie C., Musico, John Kenneth B., Pacer, Jihan S., Baniqued, Julius Rey D., Hernandez, Jaime Jr. Y., Villalba, Imee Bren O. 2021. Investigation of the Effects of the Classification of Building Stock Geometries Determined Using Clustering Techniques on the Vulnerability of Galvanized Iron Roof Covers Against Severe Wind Loading. In I*OP Conference Series: Materials Science and Engineering* 1150(1): 012024. IOP Publishing. DOI: http://dx.doi.org/10.1088/1757-899X/1150/1/012024

[8] Nishijima, Kazuyoshi, Hiroaki Nishimura, Liezl Tan, Jaime Jr. Hernandez. "Study on wind vulnerability of non-engineered houses in Leyte Island, the Philippines"

[9] Association of Structural Engineers of the Philippines. 2015."National Structural Code of the Philippines". 7th edition.

[10] Food and Agriculture Organization of the United Nation (FAO). 1997."Information Note on Asia-Pacific Forestry Sector Outlook Study".

[11] Santos, Alfonso. 2019."Empirical Study on the Changes of Pull-out Strength in A Wood Nail-Coconut Lumber Roof Connection As Affected by Weathering Conditions". Undergraduate Thesis. University of the Philippines Diliman.

[12] Acosta, Timothy John, Agar, Joshua, Gumaro, Joshua Joseph, Ereño, Mary Nathalie, Alvarez, John Phillip, Hernandez, Jaime Jr., Tingatinga, Eric Augustus, Quinay, Pher Errol, Tan, Liezl Raissa, Villalba, Imee Breen, Bisa, Harvey, Pacer, Jihan, Plamenco, Dean Ashton, Baniqued, Julius Rey, Musico, John Kenneth. 2021"Enhanced Severe Wind Vulnerability Curves of Key Building Types in the Philippines Terminal Report".

[13] Acosta, Timothy John, Carandang, Alvin Junor. 2018."Experimental Investigation of Jalousie Type Window Frames Subjected to Static Wind Pressure," *Philippine Engineering Journal*, 39(2): 75-88.

[14] Esquila, Gilfred. 2020."Vulnerability Evaluation of Wooden Planks as Wall Panels Subjected to Severe Wind Loading." Undergraduate Thesis. University of the Philippines Diliman.

[15] Tamura, Y. 2016. "Aerodynamic database for low-rise buildings." Tokyo Polytech. Univ http://wind. arch. t-kougei. ac. jp/system/eng/contents/code/tpu last accessed 9, 4 (2012):

[16] Yakhot, Victor, Steven Orszag, Siva Thangam, Thomas Gatski and Charles Speziale. 1992 "Development of turbulence models for shear flows by a double expansion technique", *Physics of Fluids A*, 4(7): 1510-1520.. DOI: https://doi.org/10.1063/1.858424

[17] Acosta, Timothy John, 2021"Risk assessment of low-rise educational buildings with wooden roof structures against severe wind loadings". Journal of Asian Architecture and Building Engineering. 1-13. DOI: https://doi.org/10.1080/13467581.2021.1909596